Physica 135B (1985) 220–223
North-Holland, Amsterdam

NEW FABRICATION TECHNIQUE AND ELECTRONIC TUNNELING STUDIES OF NbN

L.-J. LIN, E.K. TRACK, G.-J. CUI* and D.E. PROBER
Becton Center, Section of Applied Physics, Yale University, New Haven, CT 06520, USA

We have fabricated NbN films using a new dual ion-beam sputter deposition technique. In this technique, one ion beam sputters Nb from a target, while the second ion beam directly bombards the growing film. The T_c of these NbN films is typically 11–12 K when deposited on near-room temperature substrates. Preliminary results on tunneling through a native oxide barrier yield a superconducting energy gap for NbN of 1.9 meV, for which $2\Delta/kT_c = 3.9$. We have also studied oxidized overlayers of Al and Ta to produce an artificial oxide tunneling barrier. Conductance data indicate that the native oxide barrier is broad with a low barrier height (0.2–0.3 eV), whereas the oxidized Al overlayer has a higher (0.5–1.2 eV) and narrower barrier. The quality of the I–V curves for native oxide and for artificial oxide barriers is comparable.

1. Introduction

NbN is a refractory superconductor and is an attractive material for superconducting microelectronics [1–10]. It has a high T_c (16–17 K maximum) and is relatively insensitive to stress. In addition, superconducting NbN films can be deposited on unheated substrates. However, the deposition of a NbN counterelectrode to form an all high-T_c NbN–NbN junction has so far yielded reduced gap values in the counterelectrode [1, 8], possibly due to unfavorable interaction with the tunnel barrier during counterelectrode deposition. There are also a number of open scientific questions for NbN [9], including an understanding of the electron–phonon spectrum, and the origin of the very high film resistivities often reported.

The dual ion-beam sputter deposition method we have developed is intended to provide junctions which can address the issues above. First, the deposition conditions are potentially gentler (i.e., lower ion energy and/or lower temperature) than in past studies [1–10]. Previously, NbN films were produced with dc, rf or magnetron sputtering, or with high-temperature diffusion methods. There is also good control of ion energy and flux with ion-beam deposition. Recent studies have successfully produced good quality films of the materials Si_3N_4 [11] and AlN [12], using the dual ion-beam method. Second, our dual ion-beam system allows deposition of thin metallic overlayers for producing artificial oxide tunnel barriers of high quality [13, 14] as required in tunneling studies. In one previous study which used a related deposition method, a growing Nb film (deposited by electron-beam evaporation) was bombarded with N_2^+ ions [15]. Broad transitions, extending from 9–14.5 K, were reported.

In this work, we report initial success in fabricating superconducting NbN films with good but not yet ideal properties. Use of the second ion beam is found to be essential. We also find that artificial barriers of reasonable quality can be produced. We have studied barrier parameters for various combinations of materials.

2. Film preparation and properties

The sputtering configuration is shown in fig. 1. The second ion source uses N_2 or a mixture of N_2 with Kr or CH_4. Using this system, we are able to make NbN films on near-room temperature Si substrates with T_c typically 11–12 K with a transition width of ≈150 mK. Without the use of the second ion source, the films are flaky in appearance with T_c up to 11.5 K at high N_2 partial pressure. It is also found so far that high-T_c,

* On leave from Peking University, China.

0378-4363/85/$03.30 © Elsevier Science Publishing B.V.
(North-Holland Physics Publishing Division)

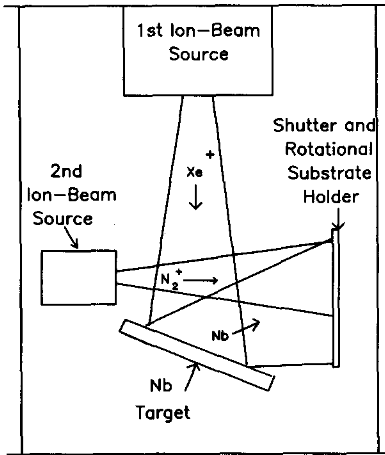

Fig. 1. Sputtering configuration. The sputtering parameters used for the first ion-beam source are $V_{beam} = 1500$ V, $I_{beam} = 34$ mA, and $P_{Xe} \approx 1.2 \times 10^{-4}$ Torr. For the second ion-beam source, the parameters are $V_{beam} = 1500$ V, $I_{beam} = 3$ mA, and $P_{N_2} \approx 0.7 \times 10^{-4}$ Torr.

single transition NbN films are produced only with high energy (>500 eV) N_2^+ flux from the second ion source. The addition of CH_4 has the potential for allowing reduced energy of the N_2^+ ions and an increased T_c.

The NbN films show non-metallic behavior, with a residual resistivity ratio ≈0.9 and resistivities of ≈150 μΩ-cm. For the films fabricated without the addition of CH_4, a Read X-ray camera identifies the structure of the film to be single-phase, δ-NbN (B1 structure). For the same films, TEM studies show polycrystalline NbN, with a grain size <100 Å. Auger (AES) analyses indicate uniform composition with a N to Nb ratio of ≈0.96 and traces of a few atomic percent of C and O.

3. Tunnel junctions

We have used the NbN films in tunnel junctions with various barriers and with evaporated $Pb_{0.71}Bi_{0.29}$ or Ag counterelectrodes. The $Pb_{0.71}Bi_{0.29}$ counterelectrode has $T_c \approx 8.35$ K with $\Delta T_c \approx 10$ mK and an extrapolated $\Delta(0) \approx 1.74$ meV [16]. The junction area is typically 3.2×10^{-4} cm^2, as defined by mechanical masks with Ge as an insulator. For most of the native oxide junctions studied, the NbN base electrode is oxidized in air for up to 4 hours at room temperature. Typical junction resistances (R_n) with native oxide barriers are on the order of a few ohms. With a $Pb_{0.71}Bi_{0.29}$ counterelectrode, we obtain SIS junctions with reasonable quality I–V curves (fig. 2), having subgap conductance (at 2 meV) ≈2% of the conductance above the gap (at 5 meV) for $T < 2$ K. The sum-gap at 1.4 K is 3.67 meV measured as the midpoint of the current rise, which extends over about 0.4 meV. This gives $\Delta_{NbN} = 1.9$ meV and $2\Delta/kT_c = 3.9$, in agreement with previous findings [3, 5, 7–9] that NbN is a strong coupled superconductor. The Josephson critical current (I_c) at 1.3 K is ≤4.5 mA, which gives a current density of ≈15 A/cm^2 and values of $I_cR_n \approx 1.2$ mV and $V_m = I_cR_{sg}(2\text{ mV}, T < 2\text{ K}) \approx 70$ mV. For junctions fabricated with a higher oxidation temperature (1 minute at 400°C), no gap feature is observed. Presumably, shorts developed while oxidizing the NbN metal [17, 18].

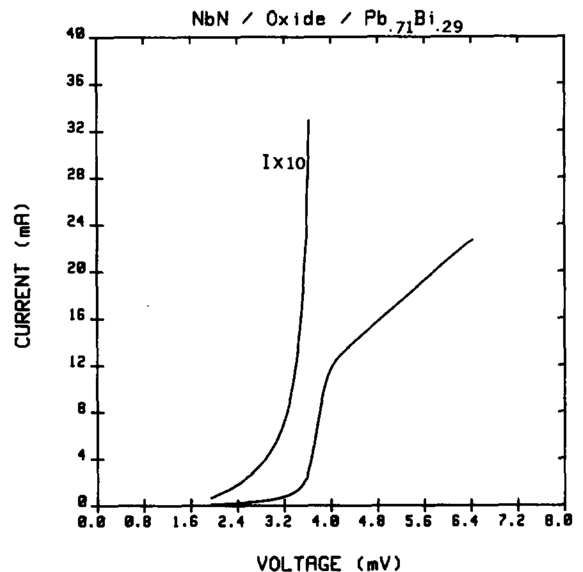

Fig. 2. I–V curves for a NbN/oxide/$Pb_{0.71}Bi_{0.29}$ junction at $T = 1.4$ K. The normal state tunneling resistance (R_n) is 0.28 Ω. The sum-gap voltage is 3.67 mV and the width of the current rise is ≈0.4 mV. The subgap conductance at 2 mV is ≈1.7% of the tunneling conductance at 5 mV.

Some of the junctions employ overlayers of Al, Ta or sequentially deposited Nb + Al or Nb + Ta. These are deposited in situ on the NbN base electrode and then air-oxidized to form artificial barriers. The quality of the *I–V* curves with overlayers, as determined by subgap leakage and the width of the tunneling current rise, is almost comparable to the native oxide junctions. However, the artificial barriers do have higher normal tunneling resistance (R_n), and the barrier heights differ significantly from those of the native oxide junctions (see below). The fact that the normalized *I–V* curves of junctions with artificial barriers are like those of the native oxide junctions may indicate that the leakage current and the width of the current rise are caused by intrinsic properties of the NbN film itself, and not the barrier.

The *I–V* curve of an overlayer junction of NbN/Nb (10 Å) + Ta (18 Å)/oxide/$Pb_{0.71}Bi_{0.29}$ has its current rise at a reduced bias voltage of 2.78 mV. This reduction is due to the proximity effect, which also causes some structure above the current rise. Use of thinner overlayers (Nb(4 Å) + Ta(9 Å), Nb(4 Å) + A1(13 Å) and A1(13 Å)) produces a much smaller or negligible depression of the voltage at which the current rise occurs.

Using a WKB analysis of the conductance vs. voltage data [19], we obtain the effective width and height of the tunneling barrier for each junction. Whereas the native NbN oxide gives low and wide barriers ($\bar{\phi} = 0.2–0.3$ eV, d_{eff} = 23–30 Å), use of an A1 overlayer yields the highest and narrowest effective barrier (table I). These results are similar to those from previous studies of Al overlayers on Nb [20].

Acknowledgements

The authors thank E.J. Cukauskas of the US Naval Research Laboratory for the Read X-ray camera study, P. Mâle for the TEM study, H. Erskine for the AES study, A. Pooley for energy dispersive X-ray analysis and D.W. Face for many helpful discussions. This work is supported in part by ONR N00014-80-C-0855 and NSF ECS 8305000, and by the APS Chinese–American Basic Research Program (for G.-J. Cui). AES studies were conducted at the University of Minnesota NSF Regional Instrumentation Facility.

References

[1] F. Shinoki, A. Shoji, S. Kosaka, S. Takada and H. Hayakawa, Appl. Phys. Lett. 38 (1981) 285.
[2] R.B. Van Dover, D.D. Bacon and W.R. Sinclair, Appl. Phys. Lett. 41 (1982) 764.
[3] D.D. Bacon, A.T. English, S. Nakahara, F.G. Peters, H. Schreiber and W.R. Sinclair, J. Appl. Phys. 54 (1983) 6509.
[4] E.J. Cukauskas, J. Appl. Phys. 54 (1983) 1013.
[5] E.J. Cukauskas, M. Nisenoff, H. Kroger, D.W. Jillie and L.N. Smith, Adv. Cryo. Eng. 30 (1984) 547.

Table I
Barrier properties of various junctions. $\bar{\phi}$ is the average barrier height, d_{eff} is the effective barrier width

Junction	Oxidation conditions	$R_n \times A$ (mΩ-cm^2)	d_{eff} (Å)	$\bar{\phi}$ (eV)
NbN/Oxide/$Pb_{0.71}Bi_{0.29}$	35 min. Air	1.8	31	0.18
NbN/Oxide/Ag	4 min. 100 mTorr O_2, 240 min. Air	1.5	23.3	0.35
NbN/Al(13 Å)/Oxide/$Pb_{0.71}Bi_{0.29}$	25 min. Air	430	18.2	1.22
NbN/Nb(4 Å) + Al(13 Å)/Oxide/$Pb_{0.71}Bi_{0.29}$	25 min. Air	1100	21.7	0.91
NbN/Nb(10 Å) + Ta(18 Å)/Oxide/$Pb_{0.71}Bi_{0.29}$	10 min. 200 mTorr O_2, 90 min. Air	3.8	18.6	0.66
NbN/Ta(9 Å)/Oxide/Ag	12 min. Air	23	23.0	0.52

[6] Y. Hoshi, N. Terada, M. Naoe and S. Yamanaka, Adv. Croy. Eng. 30 (1984) 607.
[7] M. Hikita, K. Takei and M. Igarashi, J. Appl. Phys. 54 (1983) 7066.
[8] J.C. Villegier, L. Vieux-Rochaz, M. Goniche, P. Renard and M. Vabre, IEEE Trans. Magn. MAG-21 (1985) 498.
[9] M. Gurvitch, W.L. Remeika, J.M. Rowell, J. Geerk and W.P. Lowe, IEEE Trans. Magn. MAG-21 (1985) 509.
[10] X. Wu, J. Li, T. Zhang, W. Guo and G.-J. Cui, Acta. Phys. Temp. Humilis Sinica 6 (1984) 92.
[11] C. Weissmantel, Thin Solid Films 32 (1976) 11.
[12] J.M.E. Harper, J.J. Cuomo and H.T.G. Hentzell, Appl. Phys. Lett. 43 (1983) 547.
[13] S.T. Ruggiero, D.W. Face and D.E. Prober, IEEE Trans. Magn. MAG-19 (1983) 960.
[14] S.T. Ruggiero, G.B. Arnold, E. Track and D.E. Prober, IEEE Trans. Magn. MAG-21 (1985) 850.
[15] J.J. Cuomo, J.M.E. Harper, C.R. Guarnieri, D.S. Yee, L.J. Attanasio, J. Angilello, C.T. Wu and R.H. Hammond, J. Vac. Sci. Tech. 20 (1982) 349.
[16] R.C. Dynes and J.M. Rowell, Phys. Rev. B1 (1975) 1884.
[17] P.K. Gallagher, W.R. Sinclair, D.D. Bacon and G.W. Kammlott, J. Electrochem. Soc. 130 (1983) 2054.
[18] R.P. Frankenthal, D.J. Siconolf, W.R. Sinclair and D.D. Bacon, J. Electrochem. Soc. 130 (1983) 2056.
[19] W.F. Brinkman, R.C. Dynes and J.M. Rowell, J. Appl. Phys. 41 (1970) 1915.
[20] J.M. Rowell, M. Gurvitch and J. Geerk, Phys. Rev. B24 (1981) 2278.